

CHAPTER 120

Numerical Modelling of Breaking Wave Impacts on a Vertical Wall

N. T. Wu * H. Oumeraci † H.-W. Partensky ‡

Abstract

The impact processes on a vertical wall resulting from breaking waves are numerical simulated. Two dimensional incompressible viscous flow which is governed by the Navier-Stokes Equations and the continuity equation is solved by a finite difference scheme based on the Volume of Fluid (VOF) concept. Some comparisons with experimental results reveal that the present model is able to simulate the impact process with negligible air entrainment not only qualitatively but also quantitatively well. Although the impact pressure of a plunging breaker with non-negligible air entrainment can not be quantitatively well simulated by this model due to the restriction of the incompressible flow, the wave kinematics is still well simulated.

1 Introduction

Breaking waves represent the major cause for the damage of vertical face breakwaters. The stability of such structures is in fact a dynamic problem. The solution of this problem requires among others a detailed knowledge of the impact loading; i.e. the spatial and temporal distribution of the pressure induced by the breaking waves on the structure must be determined. To date, no theoretical approach for this problem is available. On the other hand, small-scale model investigations suffer from scale effects, so that no definite quantitative conclusions can be drawn. Even results from large-scale model tests recently conducted in super-wave tanks seem to be affected to some extent by scale effects. In addition, the use of such large facilities is so expensive and so time consuming that a reasonable parameter study cannot be effectively performed. Therefore, more attention has been paid within the last 15 years to numerical methods.

Most of the existing numerical model for the simulation of breaking wave impact loads are based on potential flow theory. These methods are however unable to describe the

*Dr. -Ing., Tainan Hydraulics Laboratory, National Cheng Kung University, Tainan, Taiwan, R.O.C.

†Prof. Dr. -Ing., Univ. Professor, Techn. Univ. Braunschweig, Beethovenstr. 51a, 38106 Braunschweig, Germany

‡Prof. Dr. -Ing., Dr. phys., Prof. em. formerly Director of Franzius-Institut, Univ. Hannover, Germany

whole breaking and impact process due to the great distortion of the flow around the free surface interfaces which will not remain irrotational.

Therefore, the Volume of Fluid (VOF) (Nichols, et al., 1980) concept has been adopted here to develop a numerical model which can describe the complex free surface associated with breaking waves and the integral history of the impact pressures and forces on a vertical wall with a foreshore slope. The present paper is principally intended to present some of the results of the Ph.D. work of the first author. It will give a brief description of the developed viscous incompressible fluid model, but will particularly focus on the discussion of the results, as compared to experimental data and observations. Further developments of the model which are planned for the next years are finally outlined (air entrainment/ entrapment).

2 Governing Equations

A viscous incompressible 2D-flow is considered and the governing equations are the continuity equation:

$$\frac{\partial u}{\partial x} + \frac{\partial v}{\partial y} = 0 \quad (1)$$

and the Navier-Stokes Equations:

$$\frac{\partial u}{\partial t} + u \frac{\partial u}{\partial x} + v \frac{\partial u}{\partial y} = -\frac{1}{\rho} \frac{\partial p}{\partial x} + \nu \left(\frac{\partial^2 u}{\partial x^2} + \frac{\partial^2 u}{\partial y^2} \right) + g_x \quad (2)$$

$$\frac{\partial v}{\partial t} + u \frac{\partial v}{\partial x} + v \frac{\partial v}{\partial y} = -\frac{1}{\rho} \frac{\partial p}{\partial y} + \nu \left(\frac{\partial^2 v}{\partial x^2} + \frac{\partial^2 v}{\partial y^2} \right) + g_y \quad (3)$$

where:

ρ, ν are the density and the kinematic viscosity of the fluid, respectively.

u, v are the velocity components in x and y direction, respectively.

g_x, g_y are the x and y components of the gravitational acceleration.

p is for pressure and t is for time.

The computational domain and the boundary conditions are shown in Fig. 1. At the free surface, the pressure p should be continuous and p is therefore equal to the atmospheric pressure p_a . At the impermeable vertical wall, the free-slip condition ($\frac{\partial v}{\partial x} = 0$) and the no-flux condition ($u=0$) must be fulfilled.

For the inflow boundary conditions, any wave theory can be used to prescribe the surface elevation $\eta(t)$ and the velocity components $u(t)$ and $v(t)$. In this study, the linear wave theory, the second order solitary wave theory and the cnoidal wave theory of Keulegan and Patterson (Wiegel, 1960) are used. On the other hand, in order to keep the computational domain as small as possible, the weakly reflecting boundary condition (Delft Hydraulics, 1991) will be implemented. This allows the reflected wave to flow out the computational domain without inducing undesirable disturbance to the incident wave. The following free-slip condition for a slope is derived and considered in the model for the impermeable foreshore slope:

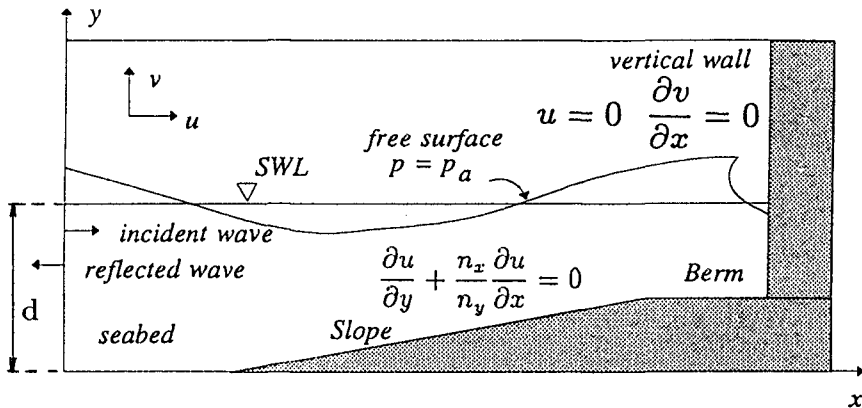


Figure 1: Computational Domain and Boundary Conditions

$$\frac{\partial u}{\partial y} + \frac{n_x}{n_y} \frac{\partial u}{\partial x} = 0 \tag{4}$$

where n_x and n_y are the components of the normal vector \vec{n} in x and y direction, respectively.

The governing equations are numerically solved by using a finite difference scheme incorporated with the Volume of Fluid (VOF) concept developed by Nichols et al. (1980) which deals with the free surface description. In this technique a function $F(x,y,t)$ which describes the fractional volume of fluid in the mesh cells is included. The free surface can therefore be described according to the value of F in the mesh cells. Besides, the kinematic free surface boundary condition can be satisfied approximately by including the following transport equation of F :

$$\frac{\partial F}{\partial t} + \frac{\partial Fu}{\partial x} + \frac{\partial Fv}{\partial y} = 0 \tag{5}$$

Physically, this means that the F function moves with the flow motion.

3 Computational Results

Nonbreaking Waves

First of all, nonbreaking waves are numerically simulated in order to verify that the present model is able to simulate correctly nonbreaking waves not only qualitatively but also quantitatively. This will then offer a reasonable working platform for simulating the more complicated breaking waves. Two cases are considered for achieving this goal, namely, solitary wave run up on a vertical wall and the formation of standing waves.

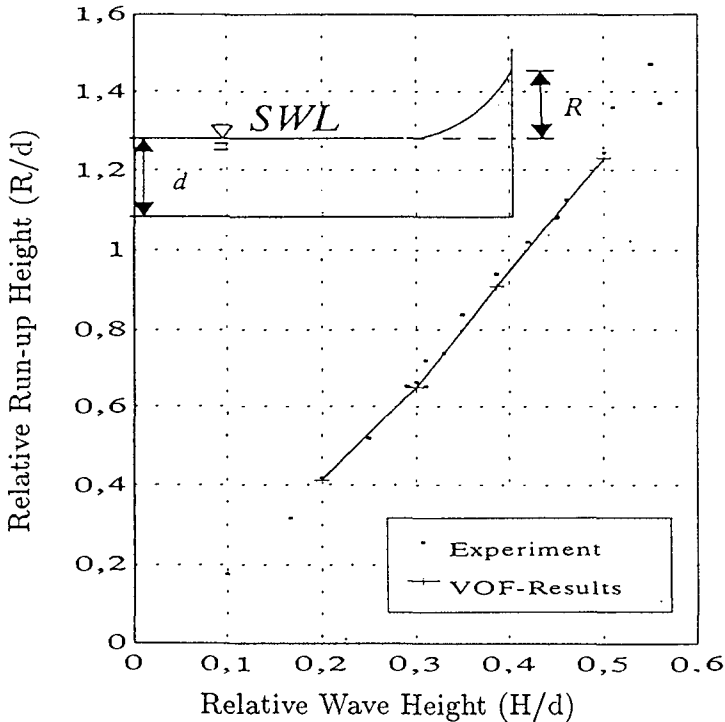


Figure 2: Comparison of Experimental and Computed Run-up Heights of Solitary Waves at a Vertical Wall

Solitary Wave Run Up on a Vertical Wall

Solitary waves propagating on a horizontal bed toward a vertical wall are first taken into account in order to verify that the free surface boundary condition is well handled in the present model. The second order solitary wave theory of Laitone(1960) is considered for incident waves. Solitary waves with relative wave heights $H/d = 0.2, 0.3, 0.4$ and 0.5 are considered. H is the wave height and d the water depth.

The computed results for the relative run up height R/d of solitary waves for different wave heights are compared with the experimental results from Street and Camfield(1966) A very good agreement between the computational and experimental results is shown in Fig. 2.

Standing Waves

In order to verify that the weakly reflecting boundary condition is well implemented in the present model, incident waves propagating toward a vertical wall with and without a foreshore slope are therefore taken into account. Due to the impermeable vertical

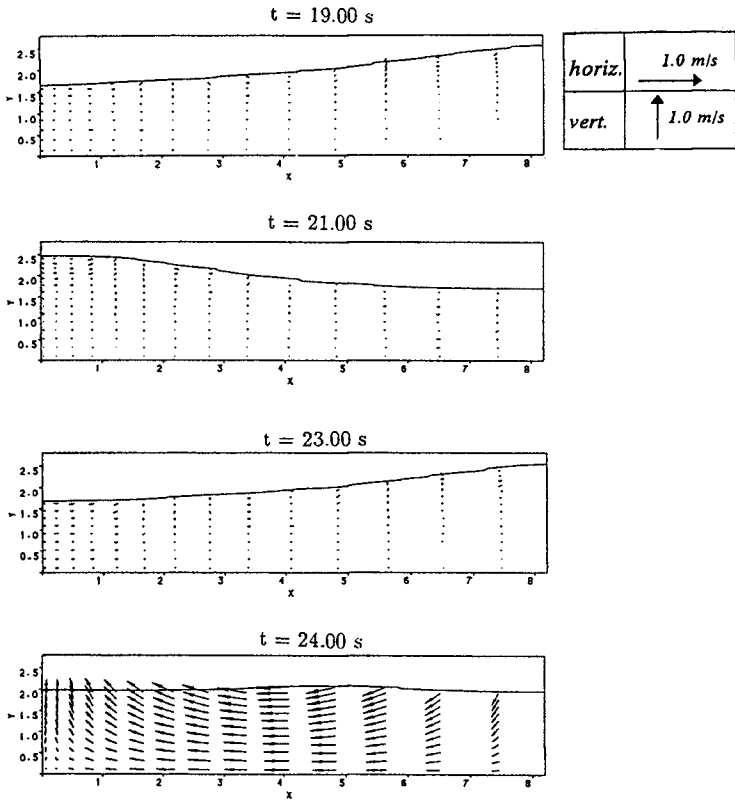


Figure 3: Numerical Simulated Standing Waves($H=0.4 \text{ m}$, $T=4.0 \text{ sec}$, $d=2.0 \text{ m}$)

wall, standing waves are expected to appear once the implemented weakly reflecting boundary condition can successfully let the reflected wave flow out the computational domain without inducing any unexpected re-reflection. The wave parameters used for this numerical test are:

- Incident Wave Height $H = 0.4 \text{ m}$; Wave Period $T = 4.0 \text{ sec}$; Water Depth $d = 2.0 \text{ m}$

Airy wave theory is used for the incident waves. The wave length can be calculated as about 16.2 m . The computational domain is $8.2 \text{ m} \times 2.8 \text{ m}$ and consists of a non-uniform grid with 40×20 cells. The antinode is located at a distance $nL/2$ ($n=0,1,2, \dots$) from the vertical wall. Therefore, the second antinode should be located near the other side of the computational domain. The numerical simulated standing wave at times $t=19.0$, 21.0 , 23.0 and 24.0 second are shown in Fig. 3. It is seen that a standing wave with also 4 second of period appeared. On the other hand, the numerically simulated pressure distribution of a standing wave on a vertical wall is compared with the theoretical

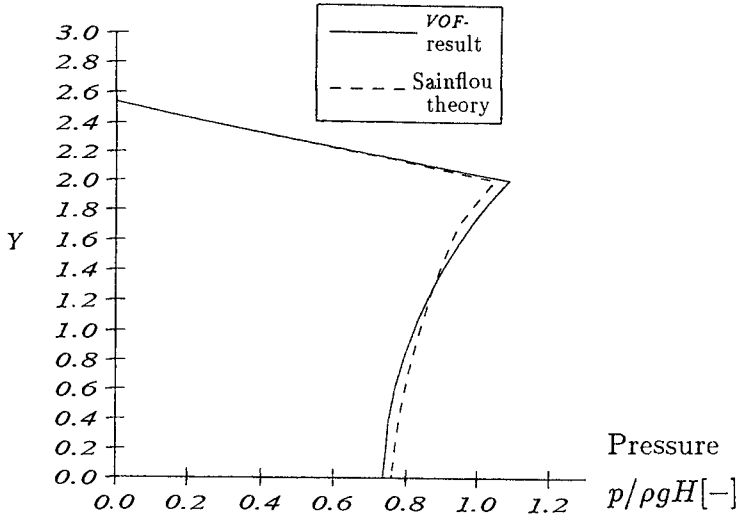


Figure 4: Pressure Distribution of Standing Wave on a Vertical Wall

results developed by Sainflou (Horikawa, 1978), and a very good agreement is shown as in Fig. 4.

Breaking Waves

Four types of breaking waves impacting on a vertical wall are distinguished by Hattori et al. (1994):

- Flip-Through type breaker
- Impact of an almost vertical breaker front on the wall with a thin air layer
- Impact of a plunging breaker on the wall with a small air pocket
- Impact of a plunging breaker on the wall with a large air pocket

The four breaker types are shown as in Fig. 5 schematically. The term "Flip-Through" was first introduced by Cooker and Peregrine (1990). This kind of impact process contains either very few or no entrapped air and the impact pressure originates from the large flow acceleration due to the concentration of flow adjacent to the vertical wall. The impact process from (b) to (d) indicates an increasing air content.

These four types of breaking waves and the resulting pressure distribution on the vertical wall are numerically simulated. The experiments by Takahashi et al. (1983) are considered for comparison, since pictures of breaking processes at different stages were recorded which can be well compared with the numerical simulated breaking processes.

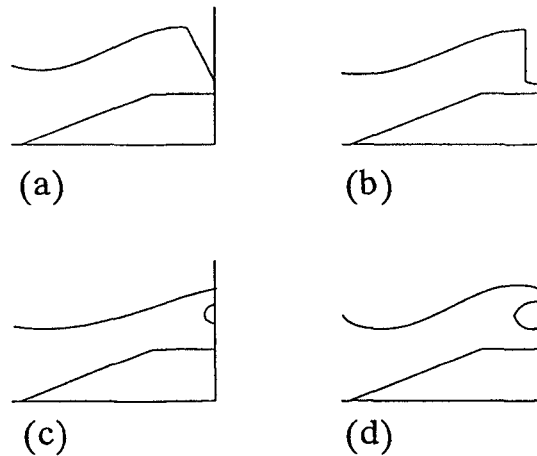


Figure 5: Schematized Breaker Types Simulated by the Numerical Model

Besides, different breaking wave impact can be systematically obtained in these experiments by simply changing the berm length in front of the vertical wall.

The wave parameters of the series of experiments which are also used for numerical simulation are

- Wave height H in front of the berm = 0.351 m
- Wave period $T = 3$ sec
- Water depth $d = 0.8$ m

The berm lengths considered in the numerical simulation are $B = 0.25$ m, 0.50 m, 0.75 m and 1.25 m, respectively. The berm height is 0.5 m and the slope is 1:10. The computational domain is 7.0 m \times 1.5 m and consists of a nonuniform grid with 150 \times 40 cells. The smallest cell width is 0.02 m and is located on the wall side and the smallest cell height is 0.02 m and is located on the mean water level.

The wave theory to be used in the numerical simulation corresponding to the wave parameters is the cnoidal wave theory. Among various existing mathematical description of cnoidal wave theories, the theory developed by Keulegan and Patterson (1940) is finally taken as the most appropriate, as recommended by Le Méhauté et al. (1968). The detailed mathematical description of the related components like the surface elevation η , the velocity components u and v etc. can be found in Wiegel(1960).

The first case to be considered is the "flip-through" type of breaking waves. The photographs recorded by Takahashi et al. (1983) refer to Photo 1(2) of the original paper. The numerical simulated breaking processes of flip-through with both of the free surface profile and velocity vector field are shown as in Fig. 6. Only a part of the computational domain is presented in this figure, x coordinate ranges from 3.5 m to 7.0 m and

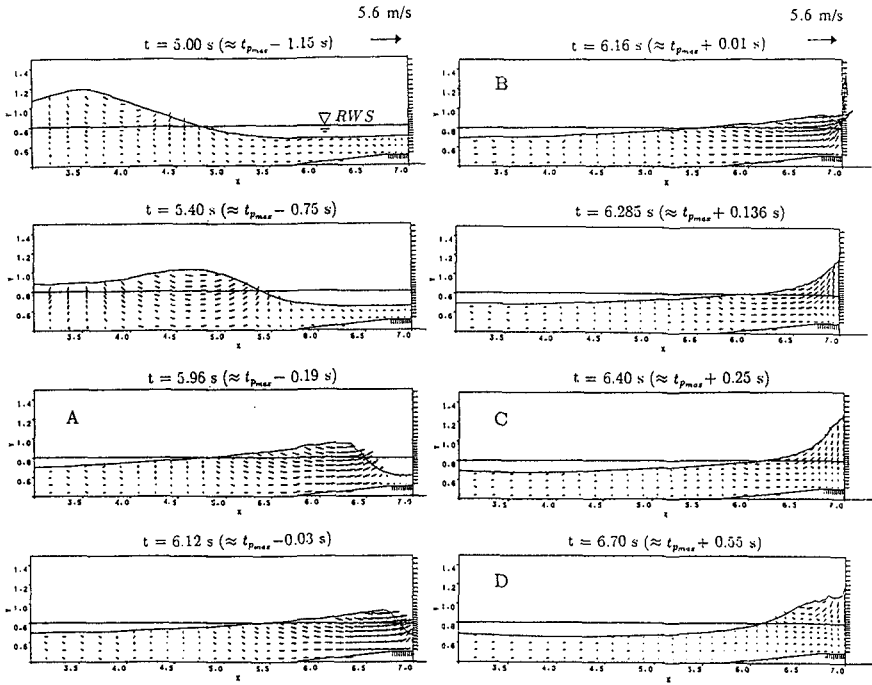


Figure 6: Computed Wave Profiles and Velocity Fields for the Flip-Through Breaker Type

the y coordinate ranges from 0.4 m to 1.5 m. After the comparison is made with the photographs taken by Takahashi et al. (1983), it is found that the numerical simulated flip through impact process agree qualitatively with the experiment.

The time history of the numerical simulated impact pressure is given in Fig. 7. The numerical simulated results agree not only qualitatively but also quantitatively well with the experimental results refer to Takahashi et al.(1983). The time history of the total force obtained by integrating the pressure distribution is shown as in Fig. 8. The characters A, B, C and D in Fig. 7 and 8 correspond to the A, B, C and D of the breaking wave processes shown in Fig. 6. It is worthwhile to mention that the point C in Fig. 8 which is the trough of the force history corresponds to the maximum run-up height of the impact process shown in Fig. 6. This phenomenon has already been pointed out experimentally by Mitsuyasu (1962) which also support the numerical simulated results.

For the other three breaker types, the numerically simulated free surface evolution of the other three breaking processes still agree qualitatively well with the photographs of the experiments. Fig. 9 is the numerical simulated breaking processes of the impact process-almost vertical breaker front with a thin air layer. The photographs of this

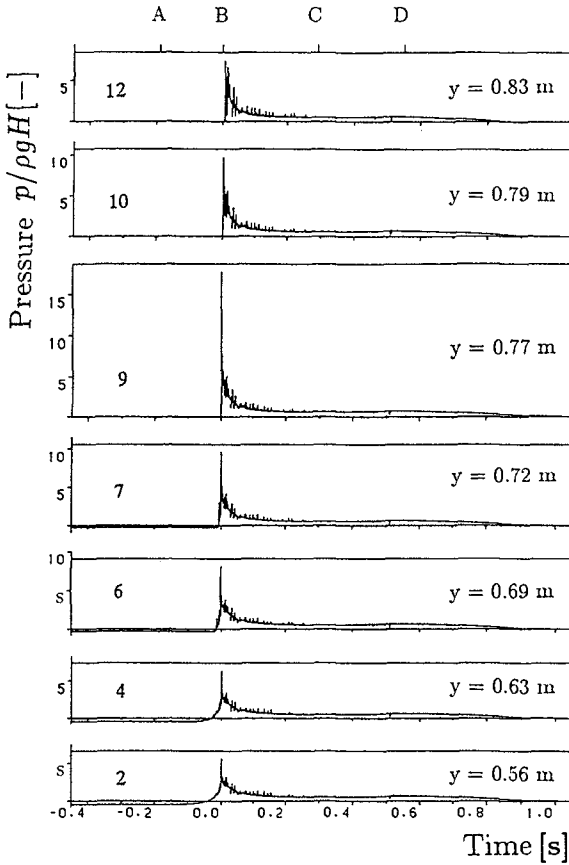


Figure 7: Computed Time History of Flip-Through Type Impact Pressure

impact process refer to Photo 1(3) of Takahashi et al. (1983). However, because the damping effect of the entrapped air can not yet be studied using the present model for incompressible flow, the resulting impact pressures of these three breaker types appear to be much larger than the experimental results and are not presented here. On the other hand, it is also found that the numerically simulated peak pressure can still be adjusted to the same order of magnitude with the experimental results once the impact velocity and breaker profiles obtained from the numerical simulation are used as the input data of Bagnold's formula which accounts for the damping effect of entrapped air. Fig. 10 are the numerical simulated free surface evolution of the plunging breaker type with small amount of air entrainment. The photographs of this impact process refer to the Photo 1(4) of Takahashi et al. (1983). Fig. 11 are the numerical simulated free surface evolution of the plunging breaker type with larger amount of air entrainment. The photographs of this impact process refer to Photo 1(5) of Takahashi et al. (1983).

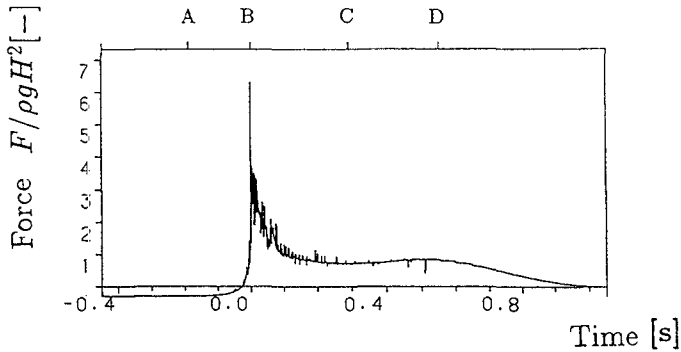


Figure 8: Computed Time History of Flip-Through Type Impact Force

On the other hand, in order to gain more insight of the computed wave kinematics of breaking waves, a comparison is made of the velocity distributions under wave crest around the breaking point. Besides, it is very difficult to define the exact breaking point during the breaking process since the free surface and velocity distribution rapidly change. It is therefore necessary to perform the comparison of experimental and numerical results under the consideration of both free surface and velocity distribution. However, this kind of measurement is rare due to the difficulty of getting an accurate velocity measurement and surface profile simultaneously. The experiment run by Iversen(1952) is still one of the most well known experiments which have considered both the surface profile and the velocity distribution. Fig. 12 shows the surface profile around the breaking point with the simultaneously observed velocity distribution. Fig. 13 shows the computed free surface around the breaking point and agrees also qualitatively well with Fig. 12. The quantitative comparison of the velocity distribution under a wave crest around breaking point is given in Fig. 14, also showing a good agreement. The X-coordinate represent the dimensionless velocity which is normalized by $\sqrt{g\eta_b}$, η_b is the water depth under the wave crest. The Y-coordinate represent the relative depth Y/η_b , $Y=1.0$ indicates the wave crest, $Y=0$ is on the bottom under the wave crest.

4 Discussion

The comparative analysis of the results of the computations may be summarized as follows:

- The basic tests of simulating non-breaking waves phenomena like the run up height of solitary waves on a vertical wall and the formation of standing waves have already proven that the present numerical model is able to correctly handling nonlinear waves and the weakly reflecting boundary.
- For flip-through breaker type (negligible air entrapment), the numerical results are qualitatively and quantitatively reliable with respect to the description of the breaker kinematics and to the subsequent impact loading on the vertical wall.

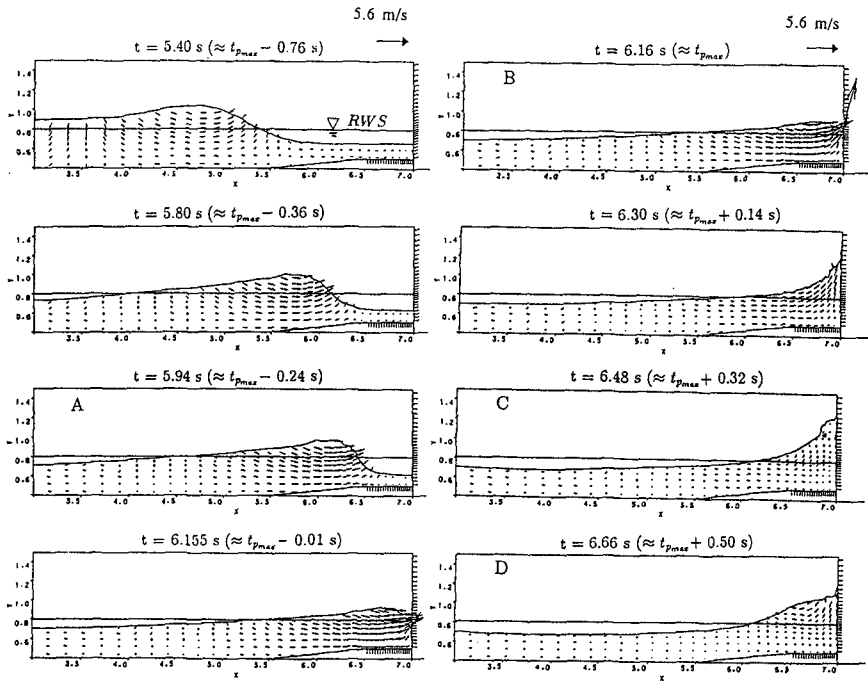


Figure 9: Computed Wave Profiles and Velocity Fields of Breaker Type- Almost Vertical Breaker Front with a Thin Air Layer

- For the last three breaker types with air entrapment in Fig. 5, the wave kinematics of the breakers is well simulated. However, the computed impact loading is much higher than the loading obtained from experiment. This result was expected since the numerical model cannot yet account for air entrapment (incompressible flow). However, by using the impact velocities and breaker profiles obtained from the numerical computation as input data into Bagnold's formula (Bagnold, 1939) which accounts for the damping effect of entrapped air, reasonable results are obtained for the magnitude of the peak impact loading.
- The last comparison is performed between the numerical simulation and the experiment done by Iversen(1952) for the velocity distribution under the wave crest around the breaking point; a quantitatively good agreement is also achieved.

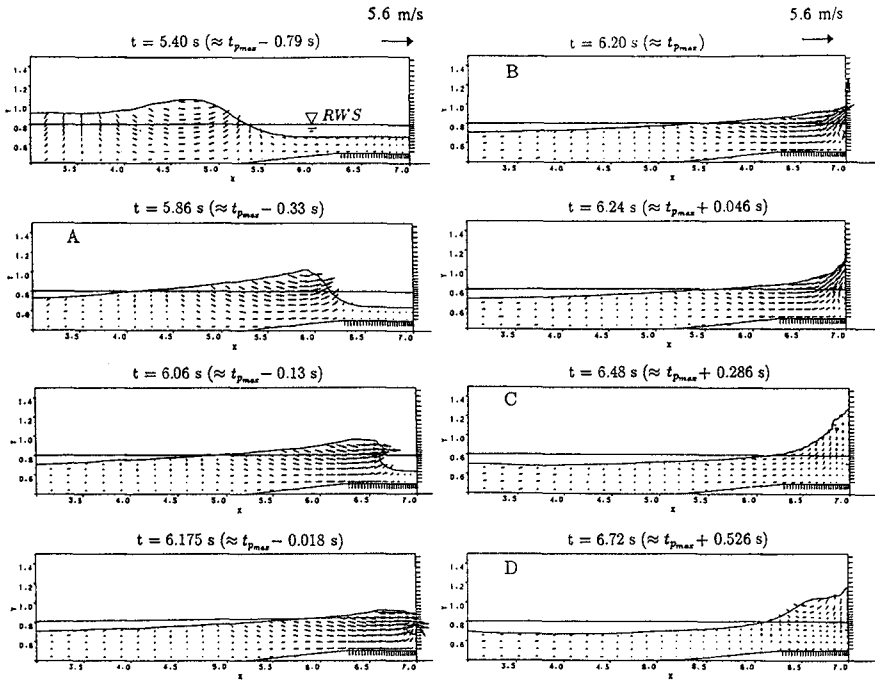


Figure 10: Computed Wave Profiles and Velocity Fields for Plunging Breaker with medium Entrapped Air Pocket

5 Concluding Remarks

The application of the VOF concept for the numerical solution of the governing equations and the development of further numerical schemes for the treatment of the boundary conditions have led to a powerful tool for the simulation of breaking and nonbreaking wave kinematics at and on a vertical structure with various foreshore geometries. The complete impact pressure and the resulting loading (impact) are also well simulated as far as the entrapped air is negligible. Corrective coefficients for the magnitude of the impact loading for the cases where air is entrapped in the breaker can be obtained from Bagnold's formula in which the impact velocity and the breaker profile during impact obtained from the numerical model are used as input data.

Further development of the model is directed towards accounting for the compressibility of air in order to obtain directly the proper magnitude of the impact loading in the case of plunging breakers with entrapped air.

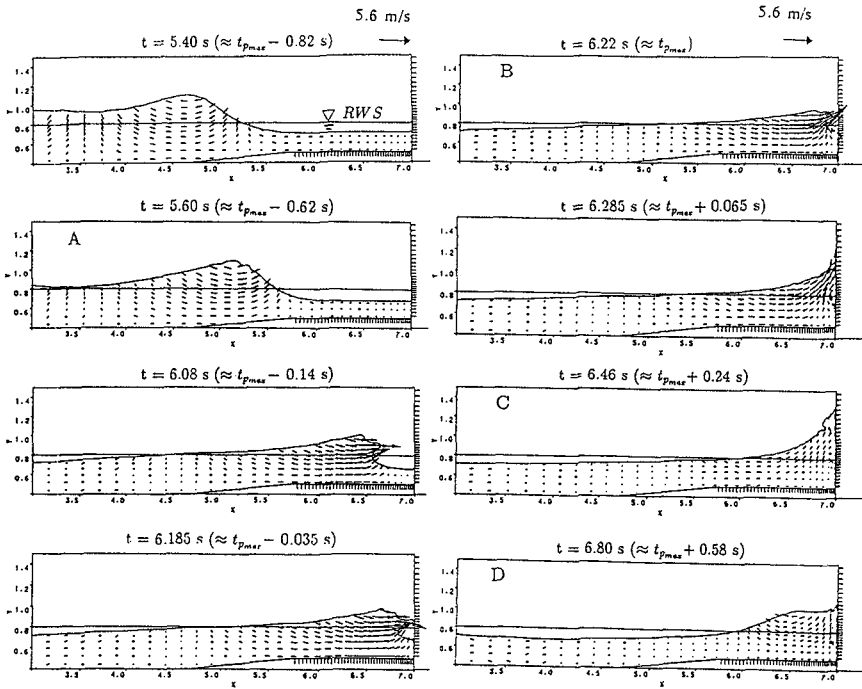


Figure 11: Computed Wave Profiles and Velocity Fields for Plunging Breaker with large entrapped airpocket

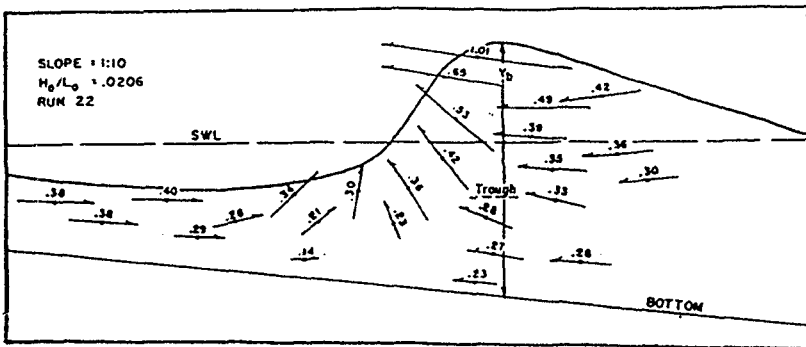


Figure 12: Surface Profile and Velocity Vectors around the Breaking Point Obtained from Experiments by Iversen(1953)

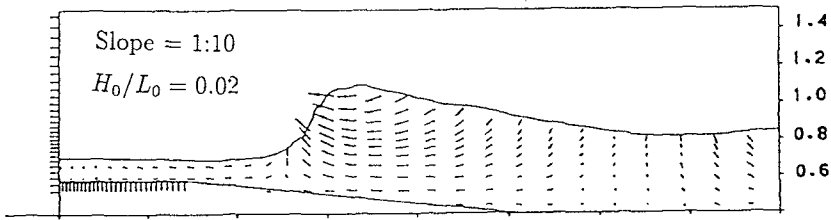


Figure 13: Surface Profile and Velocity Vectors around the Breaking Point Obtained from Numerical Simulation

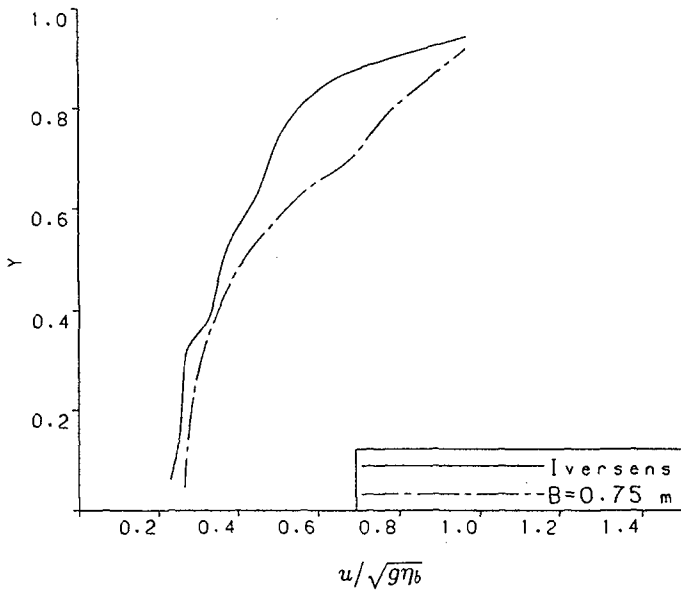


Figure 14: Comparison of Experiment and Numerical Simulation of Velocity Distribution under the Wave Crest of a Plunging Breaker

6 Acknowledgement

The first author is grateful to the Deutscher Akademischer Austauschdienst (German Scholarship Exchange Service) for awarding him the DAAD Scholarship which financially support his stay in Germany while the present study was done. The MAST II-Project MAS2-CT92-0047 supported by the EU which provided favorable research atmosphere for the development of this VOF-model is also appreciated.

7 References

1. Bagnold, R.A. (1939) Interim Report of Wave Pressure Research. J. Inst. Civil Engineers. Vol. 12, pp. 210-226.
2. Cooker, M. J. and Peregrine, D. H. (1990) Violent Water Motion at Breaking Wave Impact. Proc. 22nd Intl. Conf. on Coastal Engineering. Delft. pp. 164-176.
3. Cooker, M.J. and Peregrine, D.H. (1992) Wave Impact Pressure and its Effect upon Bodies lying on the Sea Bed. Coastal Engineering, 18. pp. 205-229.
4. Delft Hydraulics (1991) Skylla: Wave Motions in and on Coastal Structures- Feasibility Study in the Application of SAVOF- MAST G6.- Coastal Structures.
5. Hattori, M, Arami, A. Yui, T. (1994) Impact Wave Pressure on Vertical Walls under Breaking Waves of Various Types. Special Issue on Vertical Breakwaters, Coastal Engineering, Elsevier, Amsterdam.
6. Horikawa, K. (1978) Coastal Engineering- An Introduction to Ocean Engineering. University of Tokyo Press.
7. Iversen, H. W. (1952) Laboratory Study of Breakers. U.S. National Bureau of Standards, Circular No. 521 (Nov. 1952), pp. 9-31.
8. Keulegan, G. H. and Patterson, G. W. (1940) Mathematical Theory of Irrotational Translation Waves. J. Res. Natl. Bur. Std. 24.
9. Laitone, E. V. (1960) The Second Approximation to Cnoidal and Solitary Waves. J. Fluid. Mech., 9. pp. 430-444.
10. Le Méhauté, B., Divoky, D., Lin, A. (1968) Shallow Water Waves: A Comparison of Theories and Experiments. Proc. 11th Intl. Conf. on Coastal Engineering, pp. 86-107.
11. Mitsuyasu, H. (1962) Experimental Study on Wave Forces against a Wall. Coastal Engineering in Japan. Vol. 5. pp. 25-47.
12. Nichols, B.D.; Hirt, C.W.; Hotchkiss, R. S. (1980) SOLA-VOF- A Solution Algorithm for Transient Fluid Flow with Multiple Free Boundaries. Report LA-8355, Los Alamos Scientific Laboratory, University of California.
13. Street, R. L. and Camfield, F.E (1966) Observations and Experiments on Solitary Wave Deformation. Proc. 10th Intl. Conf. on Coastal Engrg, chapter 19, pp. 284-301.
14. Takahashii, S., Tanimoto, K., Suzumura, S. (1983) Generation Mechanism of Impulsive Pressure by Breaking Wave on a Vertical Wall. (in Japanese) Report of Port and Harbour Research Institute., Vol. 22, No. 4, pp. 3-31.
15. Wiegel R.L. (1960) A Presentation of Cnoidal Wave Theory for practical Application. J. Fluid Mech. 7, pp. 273-286.